

# COHERENT ANTI-STOKES RAMAN SCATTERING AS A LOCAL PROBE FOR NANOCOMPOSITE MATERIALS (NANOCARS)

S. O. Konorov,<sup>1</sup> V. P. Mitrokhin,<sup>1</sup> I. V. Smirnova,<sup>2</sup> D. A. Sidorov-Biryukov,<sup>3</sup>  
A. B. Fedotov,<sup>1,3</sup> W. Arlt,<sup>2</sup> and A. M. Zheltikov<sup>1,3\*</sup>

<sup>1</sup> Physics Department, M.V. Lomonosov Moscow State University, 119992 Moscow, Russia; E-Mail: [zheltikov@top.phys.msu.su](mailto:zheltikov@top.phys.msu.su)

<sup>2</sup> Institut für Verfahrenstechnik, Technische Universität Berlin, Strasse des 17 Juni 135, 10623 Berlin, Germany

<sup>3</sup> International Laser Center, M.V. Lomonosov Moscow State University, 119992 Moscow, Russia

**Keywords:** *nanoscale nonlinear optics, coherent anti-Stokes Raman scattering, sensing*

**Abstract:** Diagnostic aspects of coherent anti-Stokes Raman scattering (CARS) in nanocomposite materials are analyzed. The interference nature of CARS spectra and the high spatial resolution make this nonlinear process an ideal local probe for the metrology of nanostructures and nanocomposites (nanoCARS).

## Introduction:

Coherent anti-Stokes Raman scattering (CARS) [1, 2] is one of the most powerful and convenient nonlinear-optical techniques, which has been extensively used through the past four decades for gas-phase, plasma, flame, and combustion diagnostics, investigations of energy relaxation pathways in molecular systems, and high-resolution spectroscopy. More recent advances in CARS include femtosecond time-resolved measurements [3], three-dimensional microscopy [4], and coherence-controlled CARS [5].

Several nonlinear-optical techniques, such as second- and third-harmonic generation, have been recently shown to be a convenient and powerful tool for a diagnostics of nanostructured materials, allowing the detection of assemblies of nanocrystals [6] and nanotubes [7], as well as a quantitative characterization of scattering regimes in random nanocomposite materials [8]. Generally, nanoscience has benefited a lot from the integration of achievements of nanotechnologies and the capabilities of nonlinear optics [9]. In particular, specifically designed nanostructures can serve as hosts for laser-active and nonlinear-optical materials [10], leading to a new design of nanophotonic and laser-optic components.

In this work, we study coherent anti-Stokes Raman scattering from Raman-active modes of toluene molecules in solution and gas-phase nitrogen molecules infiltrated into mesoporous silica aerogels. These aerogels represent an interesting class of low-density nanocomposite materials, consisting of individual SiO<sub>2</sub> particles only a few nanometers in size, which are linked into a three-dimensional network [11]. Due to their unique properties, including a high transparency in the visible, an open mesoporous structure (with a porosity of 90--99 %), a high surface area (400--1000 m<sup>2</sup>/g), an extremely low density (0.003--0.15 g/cm<sup>3</sup>), and low thermal conductivity, silica aerogels find extensive applications as insulating materials, catalysts for chemical reactions, sound absorbers, and adsorption materials. We will demonstrate that these materials also offer several important advantages for CARS spectroscopy, serving as ideal hosts for Raman-active gases and liquids and allowing a nano-scale extension of CARS methodology, referred to as nanoCARS technique here.

## Theory of nanoCARS:

Coherent anti-Stokes Raman scattering generally involves excitation of Raman-active modes in a medium under study with a pair of pump fields with frequencies  $\omega_1$  and  $\omega_2$ . The frequency difference for these fields is tuned to a resonance with the frequency of the Raman-active mode  $\Omega$ ,

$\omega_1 - \omega_2 \approx \Omega$  (inset *I* in Fig. 1), providing a high efficiency and a high selectivity of Raman-mode excitation. The third field with a frequency  $\omega_3$  is then applied to probe coherently excited Raman modes, giving rise to an anti-Stokes signal at the frequency  $\omega_a = \omega_1 - \omega_2 + \omega_3 = \omega_3 + \Omega$  (inset *I* in Fig. 1), which is used to extract the information on the system.

CARS spectroscopy is most often employed to probe Raman-active modes of molecules, atoms, or other species in a medium of interest. Resonant features in CARS spectra, related to such Raman-active modes, are observed against a coherent background, reflecting the contribution of the nonresonant part of the cubic nonlinear-optical susceptibility. The CARS line profile is thus controlled by the interference of Raman-resonant and nonresonant parts of nonlinear-optical susceptibility,  $\chi_R^{(3)} = \chi_R^{(3)}(\omega_a; \omega_1, -\omega_2, \omega_3)$  and  $\chi_{nr}^{(3)} = \chi_{nr}^{(3)}(\omega_a; \omega_1, -\omega_2, \omega_3)$ . In the scalar theory of CARS line profiles, the intensity of the CARS signal is represented as

$$I_a \propto \left| \chi_{nr}^{(3)} + \chi_R^{(3)} \right|^2 I_1 I_2 I_3, \quad (1)$$

where  $I_1$ ,  $I_2$ , and  $I_3$  are the intensities of the pump and probe fields.

The nonresonant coherent background very often masks Raman resonances in CARS spectra, complicating CARS measurements and making CARS spectra less informative. Special polarization and coherence-control techniques have been developed to suppress the coherent background in CARS spectroscopy. The nonresonant part, on the other hand, can serve to write the phase information related to Raman modes, which would have been lost in the absence of the nonresonant components. This circumstance is extensively used in coherent Raman ellipsometry [1, 2], allowing the real and imaginary parts of the Raman-resonant cubic nonlinear susceptibility to be restored. The interference nature of CARS has been also employed earlier for  $\chi^{(3)}$  measurements for a broad class of liquids and solids [12, 13]. In what follows, we extend this technique to the metrology of nanocomposite materials.

We now extend the theory of CARS spectral interferometry to the case of a nanocomposite material consisting of two components with dielectric constants  $\varepsilon_1$  and  $\varepsilon_2$  and cubic nonlinear-optical susceptibilities  $\chi_1^{(3)}$  and  $\chi_2^{(3)}$ . The generic mixing rule for nonlinear susceptibilities is then written as [14]

$$\chi_{eff}^{(3)} = \frac{1}{f_1} \left| \frac{\partial \varepsilon_{eff}}{\partial \varepsilon_1} \right| \left( \frac{\partial \varepsilon_{eff}}{\partial \varepsilon_1} \right) \chi_1^{(3)} + \frac{1}{f_2} \left| \frac{\partial \varepsilon_{eff}}{\partial \varepsilon_2} \right| \left( \frac{\partial \varepsilon_{eff}}{\partial \varepsilon_2} \right) \chi_2^{(3)}, \quad (2)$$

where  $f_1$  and  $f_2$  are the volume filling fractions of the constituent materials and  $\varepsilon_{eff}$  is the effective dielectric constant of the nanocomposite material, which can be calculated using one of the effective-medium approaches. Although it would be of interest to consider different classes of nanocomposite materials, we will focus in what follows on the potential of CARS spectroscopy for the metrology of nanocomposite materials with an architecture of a random network of pores. This class of nanocomposites includes, in particular, nano- and mesoporous materials, as well as silica aerogels, which have been extensively employed in recent nonlinear-optical experiments. A good approximation for the effective dielectric constant for such materials is often provided by the Bruggeman formula [15],

$$f_1 \frac{\varepsilon_1 - \varepsilon_{eff}}{\varepsilon_1 + 2\varepsilon_{eff}} + f_2 \frac{\varepsilon_2 - \varepsilon_{eff}}{\varepsilon_2 + 2\varepsilon_{eff}} = 0. \quad (3)$$

We now use the mixing rule for nonlinear susceptibilities defined by Eq. (2) to demonstrate the potential of CARS spectral interferometry for the metrology of nanocomposite materials (nanoCARS). The generic idea of nanoCARS is to use a reference CARS line profile as a local probe for the parameters of a nanocomposite material. Nanocomposite materials with a random network of pores can serve as an instructive example illustrating the nanoCARS approach. We assume that the pores of our nanostructure are filled with a Raman-active medium, providing a resonant contribution to the mixing rule of Eq. (2):

$$\chi_1^{(3)} = \bar{\chi}^{(3)} g(\Delta), \quad (4)$$

where  $\Delta = (\omega_1 - \omega_2 - \Omega)/\Gamma$  is the frequency detuning of the biharmonic pump from the Raman resonance normalized to the linewidth  $\Gamma$  and  $g(\Delta)$  is a complex function describing the line profile and the phase of the resonant part of  $\chi^{(3)}$  in the bulk of the Raman-active material.

The second material in our nanocomposite structure provides a nonresonant contribution to the mixing rule (2), thus deforming the reference CARS line profile. This deformation of the CARS spectrum can be used to extract the information on the parameters of the nanostructure. We will illustrate this argument by analyzing in greater detail an important particular case of a CARS line with a Lorentzian profile, which is typical of CARS spectra of Raman vibrations in the gas phase:

$$g(\Delta) = -(i + \Delta)^{-1}. \quad (5)$$

In view of Eqs. (2), (4), and (5), the scalar-theory expression for the intensity of the CARS signal from a nanocomposite material is now written as

$$I_a \propto \left| \frac{1}{f_1} \frac{\partial \varepsilon_{\text{eff}}}{\partial \varepsilon_1} \left( \frac{\partial \varepsilon_{\text{eff}}}{\partial \varepsilon_1} \right) \frac{\bar{\chi}^{(3)} \Delta}{1 + \Delta^2} - \frac{1}{f_2} \frac{\partial \varepsilon_{\text{eff}}}{\partial \varepsilon_2} \left( \frac{\partial \varepsilon_{\text{eff}}}{\partial \varepsilon_2} \right) \chi_2^{(3)} \right|^2 + \left| \frac{1}{f_1} \left( \frac{\partial \varepsilon_{\text{eff}}}{\partial \varepsilon_1} \right)^2 \frac{\bar{\chi}^{(3)}}{1 + \Delta^2} \right|^2. \quad (6)$$

Figure 1 presents the results of calculations performed for typical parameters of a glass--air nanocomposite material with  $\varepsilon_1 = 1$  and  $\varepsilon_2 = 2.25$ . The volume filling fraction of nonresonant host material  $f_2$  is varied from 0 up to 1 in our calculations, with low  $f_2$  values (from 0.01 to 0.05) corresponding to materials with a structure similar to those of silica aerogels,  $f_2 = 1$  corresponding to a bulk host material, and  $f_2 = 0$  corresponding to the case of air with no nanostructure. We assume that the frequency difference of the pump fields is scanned through one of the Raman resonances (e.g., molecular nitrogen or oxygen in atmospheric air). We note that the deformations of the reference CARS line profile become more and more visible as the content of the nonresonant material increases in our nanostructure. These deformations of the CARS line profile are correlated with and are extremely sensitive to the changes in the contents of materials constituting the nanostructure and, hence, variations in the effective dielectric function  $\varepsilon_{\text{eff}}$  of the nanocomposite material (inset 2 in Fig. 1). The results of calculations for CARS line profiles (curves 1 - 3 in Fig. 1) and the effective dielectric function (inset 2 in Fig. 1) show that the change in the volume filling fraction  $f_2$  from 0.02 to 0.05, corresponding to the increase in the effective dielectric constant  $\varepsilon_{\text{eff}}$  from 1.018 up to 1.045, leads to a dramatic change in the CARS line profile (cf. curves 2 and 3 in Fig. 1), demonstrating the possibility to use CARS line profiles for probing local inhomogeneities in the effective parameters of nanocomposite materials.

Obviously, in contrast to CARS microscopy [4], designed to resolve individual micro-objects, nanoCARS cannot resolve individual nanocrystals in a nanocomposite material, but it can locally probe the effective-medium linear and nonlinear-optical properties of a nanostructure. The spatial resolution of this method of nanostructure metrology is determined by the CARS interaction volume, which can be made less than a micrometer in diameter and a few micrometers in length in the case of tightly focused noncollinear pump beams.

## Experimental:

The synthesis of aerogels is generally based on the hydrolysis of metal alkoxide by reaction with water in the presence of alcohol and catalyst. The hydrolyzed metal alkoxide undergoes a condensation reaction, forming a metal oxide gel, from which solvents are supercritically extracted to form an aerogel. Supercritical extraction preserves the three-dimensional structure of silica gels, preventing shrinkage and providing an open mesoporous structure with a high porosity 90-99 %, a high surface area, and an extremely low density [16].

The laser system employed in our experiments consisted of a  $Q$ -switched Nd: YAG master oscillator, Nd: YAG amplifiers, frequency-doubling crystals, a dye laser, as well as a set of totally reflecting and dichroic mirrors and lenses adapted for the purposes of CARS experiments. The  $Q$ -switched Nd: YAG master oscillator generated 15-ns pulses of 1.064- $\mu\text{m}$  radiation, which were then amplified up to about 5 mJ by a Nd: YAG amplifier. Fundamental radiation was then converted into the second harmonic with a KDP crystal. The second harmonic produced in this

crystal served as one of the pump beams in the CARS process (fixed frequency  $\omega_1$ ). Fundamental radiation that remained frequency-unconverted at the output of the KDP crystal was separated from the second harmonic with a dichroic mirror and employed to generate the second harmonic in the second KDP crystal. This second-harmonic beam was then used to pump a frequency-tunable dye laser. Dye-laser radiation served as the second pump beam in the CARS process (tunable frequency  $\omega_2$ ). A dichroic mirror was used to couple spherically focused laser beams with the frequencies  $\omega_1$  and  $\omega_2$  into a silica aerogel sample at an angle of about  $30^\circ$  with respect to each other.

Two types of Raman-active species were studied in our experiments. Toluene solution was employed as an example of a liquid-phase Raman-active substance infiltrated into silica aerogel. Molecular nitrogen from the atmospheric air filling the pores of silica aerogel samples under normal conditions served to demonstrate the possibility of nanoCARS gas-phase sensing. The frequency difference  $\omega_1 - \omega_2$  was scanned through the frequencies of  $1004\text{-cm}^{-1}$  vibrations of toluene and  $2331\text{-cm}^{-1}$  vibrations of nitrogen molecules. The CARS signal, generated at the frequency  $\omega_{\text{CARS}} = 2\omega_1 - \omega_2$  in the noncollinear geometry in the beam interaction area, was collimated with a spherical lens, separated from the pump and probe beams with a set of optical filters, dispersed with a monochromator, and detected with an optical multichannel analyzer. The energy of the second-harmonic pulse was varied in the range of  $0.1 - 4$  mJ in CARS experiments, while the energy of dye-laser radiation ranged from  $0.1$  up to  $0.8$  mJ.

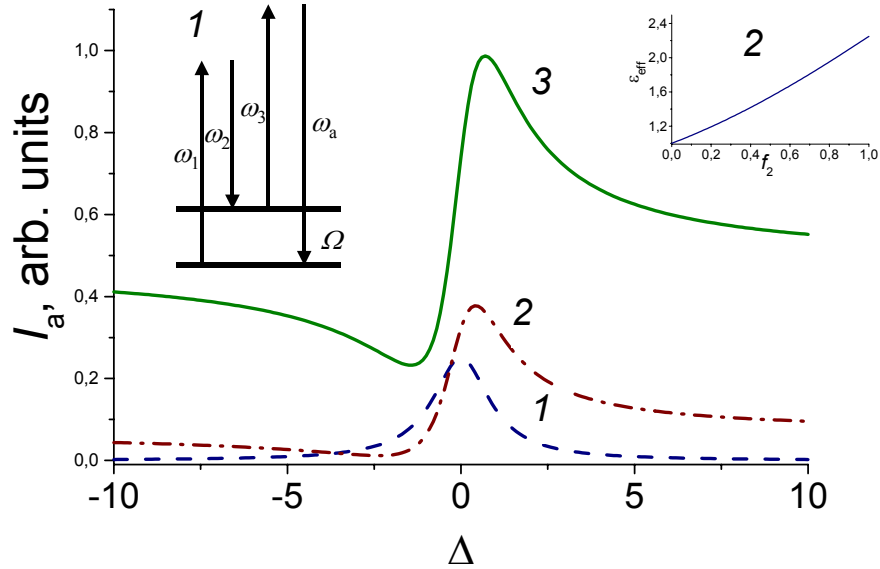


Fig. 1. Intensity of the CARS signal from a nanostructure consisting of two materials with dielectric constants  $\epsilon_1 = 1$  and  $\epsilon_2 = 2.25$ , the volume filling fractions  $f_1$  and  $f_2 = 1 - f_1$ , and third-order nonlinear susceptibilities  $\chi_1^{(3)} = -\bar{\chi}^{(3)}/(i + \Delta)$  and  $\chi_2^{(3)}$  calculated as a function of the normalized frequency detuning from the Raman resonance,  $\Delta = (\omega_1 - \omega_2 - \Omega)/\Gamma$ , for  $|\bar{\chi}^{(3)}|/|\chi_2^{(3)}| = 0.01, f_2 = 0$  (curve 1),  $0.02$  (2), and  $0.05$  (3). The insets show the diagram of the CARS process (1) and the effective dielectric constant of the nanocomposite material as a function of the volume filling fraction  $f_2$  (2).

### Results and discussion:

Toluene solution and gas-phase molecular nitrogen represent two classes of Raman-active media in a nanocomposite host, illustrating two radically different regimes of CARS in a nanostructure environment. In the case of  $1004\text{-cm}^{-1}$  vibrations in toluene solution, the Raman-resonant nonlinearity  $|\bar{\chi}^{(3)}|$ , responsible for the CARS process, is typically substantially higher than the nonlinearity of the host material  $\chi_{nr}^{(3)}$ , with the ratio  $|\bar{\chi}^{(3)}|/|\chi_{nr}^{(3)}|$  estimated as  $20\text{--}100$  for the

reagent-grade toluene sample used in our experiments. CARS spectra display characteristic symmetric profiles in this regime (Fig. 2A), indicating the dominant contribution of the resonant part of the nonlinear-optical susceptibility. The cubic nonlinear optical susceptibility related to  $2331\text{-cm}^{-1}$  vibrations of gas-phase molecular nitrogen in the atmospheric air filling the pores of silica aerogel is, on the other hand, much lower than the nonresonant contribution related to the solid-state nanostructured host,  $|\bar{\chi}^{(3)}|/|\chi_{nr}^{(3)}| \approx 0.001 - 0.005$ . Still, due to the high porosity of the host, the contribution of Raman-resonant vibrations of gas-phase molecular nitrogen is easily detectable (Fig. 2B), suggesting silica aerogels as promising materials for the creation of gas- and condensed-phase sensors of chemical and biological species, including sensors of pollutants and aerosols. The interference of resonant and nonresonant parts of the nonlinear polarization of the nanocomposite material results in an asymmetric CARS line profile in this case. For comparison, the dashed line in Fig. 2B shows the CARS spectrum of the same line measured for molecular nitrogen in free atmospheric-pressure air. With no contribution of the nanostructured host, the CARS line profile, as resolved by our spectrometer, is symmetric, showing no interference fringes typical of the nanoCARS signal. Local-field effects, typical of nanocomposite materials [17], can, on the other hand, substantially enhance nonlinear-optical interactions in silica aerogel hosts, as it was earlier demonstrated for other porous materials [10, 18], serving to improve the sensitivity of nanoCARS metrology.

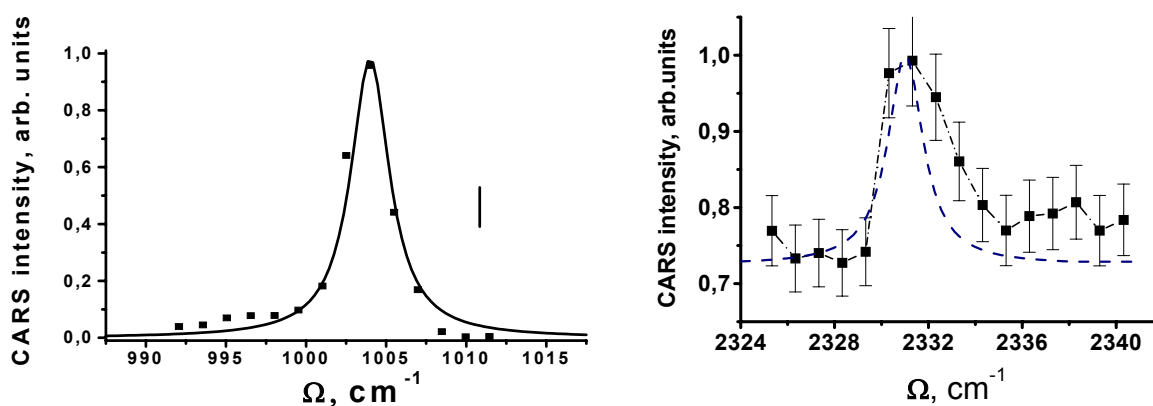


Fig. 2. A: The spectrum of the CARS signal from reagent-grade toluene infiltrated into a silica aerogel sample with an air filling fraction of 97%. The line is the guide for the eye.  
 B: The spectrum of the CARS signal from Raman-active vibrations of molecular nitrogen in free atmospheric-pressure air (dashed line) and in the atmospheric air filling the pores of the silica aerogel host with an air filling fraction of 97%. The dash--dotted line is the guide for the eye.

### Conclusion:

Experimental studies and theoretical analysis performed in this paper reveal a high potential of coherent anti-Stokes Raman scattering as a diagnostic tool for nanocomposite materials. We have demonstrated, in particular, efficient coherent anti-Stokes Raman scattering from Raman-active modes of toluene molecules in solution and gas-phase nitrogen molecules infiltrated into mesoporous silica aerogels. The interference nature of CARS spectra and the high spatial resolution make this nonlinear process an ideal local probe for the metrology of nanostructures and nanocomposites. In contrast to CARS microscopy, intended to resolve individual micro-objects, the coherent Raman spectral interferometric technique proposed here and referred to as nanoCARS, cannot resolve individual nanocrystals in a nanocomposite material, but it can locally probe the effective-medium linear and nonlinear-optical properties of a nanostructure. The spatial resolution of this method is determined by the CARS interaction volume, which can be made less than a micrometer in the case of tightly focused noncollinear pump beams. Due to a combination of remarkable properties, including their high porosity, high transparency in the visible, and weak

scattering, silica aerogels provide an ideal host for Raman-active gases and liquids, detected and analyzed by coherent anti-Stokes Raman scattering, allowing the creation of gas- and condensed-phase sensors of chemical and biological species, including sensors of pollutants and aerosols, and suggesting an interesting nano-scale extension of CARS methodology.

### Acknowledgments:

Illuminating discussions with P.K. Kashkarov, L.A. Golovan, V.Yu. Timoshenko, and S.V. Zaboltnov are gratefully acknowledged. This study was supported in part by the President of Russian Federation Grant MD-42.2003.02, the Russian Foundation for Basic Research (projects nos. 03-02-16929 and 02-02-17098), and INTAS (projects nos. 03-51-5037 and 03-51-5288). The research described in this publication was made possible in part by Award no. RP2-2558 of the U.S. Civilian Research & Development Foundation for the Independent States of the Former Soviet Union (CRDF). This material is also based upon work supported by the European Research Office of the US Army under Contract No. 62558-03-M-0033.

### References:

1. S.A. Akhmanov and N.I. Koroteev, *Methods of Nonlinear Optics in Light Scattering Spectroscopy* (Nauka, Moscow, 1981) (in Russian).
2. G.L. Eesley, *Coherent Raman Spectroscopy* (Pergamon, Oxford, 1981).
3. *Femtosecond Coherent Raman Spectroscopy*, Special Issue of J. Raman Spectrosc. **31**, nos. 1/2 (2000), ed. by W. Kiefer.
4. A. Zumbusch, G.R. Holton, and X. Sunney Xie, *Phys. Rev. Lett.*, **82**, 4142 (1999).
5. N. Dudovich, D. Oron, and Y. Silberberg, *Nature* **418**, 512 (2002).
6. S. O. Konorov, A. B. Fedotov, A. A. Ivanov, M. V. Alfimov, S. V. Zaboltnov, A. N. Naumov, D. A. Sidorov-Biryukov, A. A. Podshivalov, A. N. Petrov, L. Fornarini, M. Carpanese, G. Ferrante, R. Fantoni, and A. M. Zheltikov, *Opt. Commun.* **224**, 309 (2003).
7. D. A. Akimov, M. V. Alfimov, S. O. Konorov, A. A. Ivanov, S. Botti, A. A. Podshivalov, R. Ciardi, L. De Dominicis, L. S. Asilyan, R. Fantoni, and A. M. Zheltikov, *J. Exp. Theor. Phys.* **98**, 220 (2004).
8. S. O. Konorov, D. A. Sidorov-Biryukov, I. Bugar, J. Kovač, L. Fornarini, M. Carpanese, M. Avella, M. E. Errico, D. Chorvat Jr., J. Kovač Jr., R. Fantoni, D. Chorvat, and A. M. Zheltikov. *Appl. Phys. B* **78**, 73 (2004).
9. *Nonlinear Optics of Photonic Crystals*, Feature issue of the Journal of Optical Society of America B **19**, no. 9 (2002), ed. by C. M. Bowden and A. M. Zheltikov.
10. P.K. Kashkarov, L.A. Golovan, A.B. Fedotov, A.I. Efimova, L.P. Kuznetsova, V.Yu. Timoshenko, D.A. Sidorov-Biryukov, A.M. Zheltikov, and J.W. Haus, *J. Opt. Soc. Am. B* **19**, 2273 (2002).
11. Aerogels, ed. J. Fricke, Springer, Berlin, 1986
12. M. D. Levenson, C. Flytzanis, and N. Bloembergen, *Phys. Rev. B* **6**, 3962 (1972).
13. M. D. Levenson and N. Bloembergen, *Phys. Rev. B* **10**, 4447 (1974).
14. X.C. Zeng, D.J. Bergman, P.M. Hui, and D. Stroud, *Phys. Rev. B* **38**, 10970 (1988).
15. D. A. G. Bruggeman, *Ann. Phys.* **24**, 636 (1935).
16. I. Smirnova and W. Arlt, *J. Sol-Gel Sci. Technol.* **28**, 175 (2003).
17. J.E. Sipe and R.W. Boyd, *Phys. Rev. A* **46**, 1614 (1992).
18. S. V. Zaboltnov, A. B. Fedotov, S. O. Konorov, T. V. Veselova, I. E. Smirnova, P. K. Kashkarov, and A. M. Zheltikov, *Opt. Commun.* **229**, 397 (2004).